

## Article

# Climate Change Facilitates the Potentially Suitable Habitats of the Invasive Crop Insect *Ectomyelois ceratoniae* (Zeller)

Changqing Liu <sup>1,2,†</sup>, Ming Yang <sup>2,†</sup>, Ming Li <sup>2</sup>, Zhenan Jin <sup>2</sup>, Nianwan Yang <sup>2,3</sup> , Hao Yu <sup>1,\*</sup> and Wanxue Liu <sup>2,\*</sup>

<sup>1</sup> Department of Natural Resources, Henan Institute of Science and Technology, Xinxiang 453003, China; lcq0321@163.com

<sup>2</sup> State Key Laboratory for Biology of Plant Diseases and Insect Pests, Institute of Plant Protection, Chinese Academy of Agricultural Sciences, Beijing 100193, China; y1750165592@163.com (M.Y.); 11763650355m@163.com (M.L.); jinzhenan0308@163.com (Z.J.); yangnianwan@caas.cn (N.Y.)

<sup>3</sup> Institute of Western Agriculture, Chinese Academy of Agricultural Sciences, Changji 831100, China

\* Correspondence: yuhao971222@163.com (H.Y.); liuwanxue@caas.cn (W.L.)

† These authors contributed equally to this work.

**Abstract:** Invasive alien insects directly or indirectly driven by climate change threaten crop production and increase economic costs worldwide. *Ectomyelois ceratoniae* (Zeller) is a highly reproductive invasive crop insect that can severely damage fruit commodities and cause significant economic losses globally. Estimating the global potentially suitable habitats (PSH) of *E. ceratoniae* is an important aspect of its invasive risk assessment and early warning. Here, we constructed an optimized MaxEnt model based on the global distribution records of *E. ceratoniae*, and nine environmental variables (EVs), to predict its global PSH under current and future climates. Our results showed that the RM value was 2.0 and the mean area under receiver operating characteristic curve (AUC) value was 0.972, indicating the high accuracy of the optimal MaxEnt model. The mean temperature of driest quarter (bio9, 50.2%), mean temperature of wettest quarter (bio8, 16.9%), temperature seasonality (bio4, 9.7%), and precipitation of coldest quarter (bio19, 9.1%) were the significant EVs affecting its distribution patterns. The global PSH of *E. ceratoniae* are mainly located in western Asia under current climate scenarios ( $687.57 \times 10^4 \text{ km}^2$ ), which showed an increasing trend under future climate scenarios. The PSH of *E. ceratoniae* achieved the maximum under the shared socioeconomic pathway (SSP) 1–2.6 in the 2030s and under the SSP2–4.5 in the 2050s. The increased PSH of *E. ceratoniae* are mainly located in southwestern Asia, northwestern Europe, northwestern South America, northwestern North America, southern Oceania, and northwestern Africa. Our findings suggest that quarantine officials and governmental departments in the above high-risk invasion areas should strengthen monitoring and early warning to control *E. ceratoniae*; in particular, cultural measures should be taken in areas where its further expansion is expected in the future.

**Keywords:** climate change; *Ectomyelois ceratoniae*; MaxEnt; potentially suitable habitats



**Citation:** Liu, C.; Yang, M.; Li, M.; Jin, Z.; Yang, N.; Yu, H.; Liu, W. Climate Change Facilitates the Potentially Suitable Habitats of the Invasive Crop Insect *Ectomyelois ceratoniae* (Zeller). *Atmosphere* **2024**, *15*, 119. <https://doi.org/10.3390/atmos15010119>

Academic Editors: Shengpei Dai and Zhizhong Zhao

Received: 13 December 2023

Revised: 9 January 2024

Accepted: 16 January 2024

Published: 19 January 2024



**Copyright:** © 2024 by the authors. Licensee MDPI, Basel, Switzerland. This article is an open access article distributed under the terms and conditions of the Creative Commons Attribution (CC BY) license (<https://creativecommons.org/licenses/by/4.0/>).

## 1. Introduction

With the increase in global trade and human activities, climate change and biological invasion is becoming increasingly frequent and has become one of the high-ranking worldwide environmental problems in the twenty-first century [1]. Invasive alien insects have become an important part of biological invasion due to their robust adaptability for both reproduction and dispersal, which can reduce crop yield, decrease species richness, cause significant economic losses in invaded areas, and pose hazards to human health. These insects are a research hotspot, being one of the most extensively and best-studied groups of current research [2]. Lepidoptera is the second largest order of insects and many of its members are globally important agricultural pests that pose a significant threat to agricultural production. For example, Lepidoptera causes direct damage to fruit and may affect the quality, yield, or both, of harvestable produce [3]. *Conogethes punctiferalis* (Guenée) damaged

20% of the fruits in Jammu and Kashmir, which led to a 50% reduction in grape production in Karnataka [4,5]. Furthermore, climate change will breakdown temperature barriers to growth and dispersal that limit the range of movement of many insects, as well as facilitate the global invasion of invasive alien insects and change their global geographic distribution patterns [4,6]. Consequently, estimating the potentially suitable habitats (PSH) of invasive alien insects under climate change is critical for their monitoring, control, and management.

*Ectomyelois ceratoniae* (Zeller) (Lepidoptera) is a highly polyphagous insect that affects numerous hosts, including pomegranate, date palm, citrus, and figs [7]. It is originally from the Mediterranean region and is widely distributed across six continents, due to its accidental introduction as a contaminant crop [8,9]. The phytophagous larval stage of *E. ceratoniae* can damage the leaves, shoots, and fruits of host plants [3]. Its larvae can enter the fruit from the corolla or use fissures in the pericarp to enter the fruit and cause damage [10]. Adult females lay their eggs in the corolla of the host plant or in the cracks in the peel, which rot internally, leading to contamination by saprophytic fungi [11]. It not only reduces fruit production, but also causes economic losses. For example, *E. ceratoniae* invasion caused losses in the yield of pomegranate and date palm fruit of >80% in Tunisia [12]. In California, infested fruits can be damaged, yielding 10–40% of the harvestable crop each year; over USD 1 million is spent annually to prevent *E. ceratoniae* damage to fruit [13]. Therefore, some countries have added it to the quarantine list to prevent its further spread. For example, it has been recorded on the list of imported plant quarantine pests by the Ministry of Agriculture and Rural Affairs of the People's Republic of China since 2007. However, previous research has focused on the biological characteristics and control measures of *E. ceratoniae* [12,14–19], and few have investigated the PSH of *E. ceratoniae* under climate change. Only a few studies have frequently used the maximum entropy method (MaxEnt) models to predict the current and future distribution of other Lepidopterous pests, such as *Cydia pomonella* (Linnaeus) and *Cadra figulilella* (Gregson) [20,21]. Considering the wide spread of *E. ceratoniae* and its serious threat to fruit production [22,23], predicting the PSH of *E. ceratoniae* is beneficial for early warning and control on a global scale.

Species distribution models (SDMs) are considered one of the most important tools for predicting species distribution and population dynamics in ecology and biogeography [24–26] and include CLIMEX, BIOCLIM, genetic algorithm for rule-set prediction (GARP), generalized linear models (GLM), and MaxEnt [7,27–29]. MaxEnt, a generalized machine learning method [30,31], is the most commonly used to predict PSH for invasive species. For example, MaxEnt models have been used to study the PSH of invasive alien species *Parapediasia teterrella* (Zincken) in East Asia [32] and *Agrotis robusta* (Blanchard) worldwide [33]. Compared with other SDMs, it has the advantages of shorter running time, smaller sample size required, and higher accuracy. In addition, it is effective for most taxa and outperforms other models in terms of the accuracy of predictions, particularly when species distribution data are incomplete [34,35]. However, using MaxEnt with default parameter settings probably leads to model overfitting, which can be effectively optimized using the ENMevals v2.0.4 package [36,37]. Therefore, our study used the optimized MaxEnt model to predict the PSH of *E. ceratoniae* under current and future climate scenarios.

In the present study, we used the optimal MaxEnt model to predict the PSH of *E. ceratoniae* under current and future climate scenarios in the 2030s and 2050s. We aimed to (1) identify the important environmental variables (EVs) affecting the PSH of *E. ceratoniae*; (2) predict the PSH of *E. ceratoniae*; (3) analyze the changes in the PSH of *E. ceratoniae* under different future climate scenarios; and (4) analyze the PSH center transfer trend of *E. ceratoniae* from current to future climate scenarios. These results provide an important theoretical foundation for preventing the further expansion and population establishment of *E. ceratoniae*.

## 2. Materials and Methods

### 2.1. Distribution Records of *Ectomyelois ceratoniae*

A total of 327 *E. ceratoniae* distribution records were collected from several databases, including the Global Biodiversity Information Facility (GBIF: <https://doi.org/10.15468/dl.73j6ct>; accessed on 26 August 2022) [38], China National Knowledge Infrastructure (CNKI: <https://www.cnki.net/>; accessed on 27 May 2022), and the Web of Science (WOS: <https://www.webofscience.com/>; accessed on 7 June 2022). Distribution records without clear geographical information and duplicate records were excluded. To avoid overfitting, we used the ENMTools v1.3 to maintain only one distribution record for each  $5 \times 5$  km raster [36,39]. Finally, 228 global distribution records of *E. ceratoniae* were obtained for modeling its PSH with MaxEnt model (Figure 1).

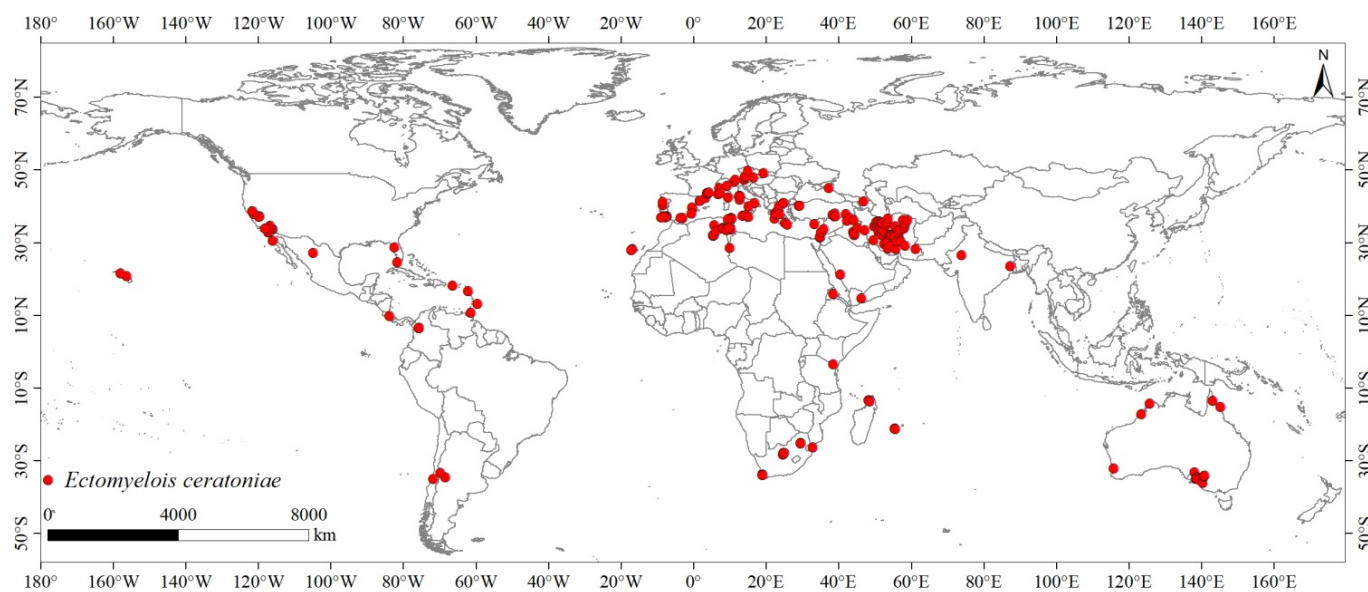


**Figure 1.** Global distribution points of *Ectomyelois ceratoniae*.

### 2.2. Environmental Variables

Nineteen EVs with 2.5 min under current climate data (1971–2000) and future climate data (2021–2040 and 2041–2060) were obtained from the World Climate Database (Table S1) [40]. Future climate scenarios include SSP1-2.6, SSP2-4.5, and SSP5-8.5, which simulate the lowest-level, moderate-level and highest-level greenhouse gas emission scenarios.

The presence of multicollinearity between EVs can lead to model overfitting. To avoid this problem, we analyzed the correlation coefficients between the 19 EVs via the Pearson correlation coefficient [41] and used 10 repeated runs of the MaxEnt model to eliminate non-contributing EVs. We retained one with a higher contribution rate in both EVs when the coefficient of correlation in two EVs was greater than 0.8 ( $|r| \geq 0.8$ ) [42] (Figure S1). Finally, we retained 9 EVs to run the MaxEnt model (Table 1).

**Table 1.** Contribution of significant environmental variables (EVs).

Variable	Description	Contribution (%)
bio9	Mean temperature of driest quarter (°C)	50.2
bio8	Mean temperature of wettest quarter (°C)	16.9
bio4	Temperature seasonality (standard deviation $\times$ 100) (°C)	9.7
bio19	Precipitation of coldest quarter (mm)	9.1
bio15	Precipitation seasonality (coefficient of variation)	3.6
bio18	Precipitation of warmest quarter (mm)	3.6
bio13	Precipitation of wettest month (mm)	2.9
bio2	Mean diurnal range (Mean of monthly (max temp–min temp)) (°C)	2.3
bio17	Precipitation of driest quarter (mm)	1.7

### 2.3. Model Calibration, Construction, and Evaluation

Feature combinations (FCs) and regularization multiplier (RM) are significant evaluation criterion to construction the MaxEnt model [43]. FCs contains five features: linear (L), quadratic (Q), fragmented (H), product (P), and threshold (T). We chose six combinations of FCs, including L, LQ, H, LQH, LQHP, and LQHPT, respectively, and the RM was set from 0.5 to 4 with an interval of 0.5. The ENMeval package via Rstudio was used to optimize the RM and FCs parameters in 48 combinations to calibrate the MaxEnt model [36,37]. When the delta Akaike information criterion correction ( $\Delta AICc$ ) was the minimum value, we chose the FCs and RM to set the MaxEnt model [44].

In this study, 228 global distribution records of *E. ceratoniae* and nine EVs were used to run the optimized MaxEnt model. Out of all *E. ceratoniae* distribution records, about 25% were selected as the test set, and the remaining records were used as the training set. The maximum number of iterations was set at 500, and the maximum number of background points was set to 10,000 with 10 repetitions [45]. The output format was set to Cloglog, and the validation type was set to bootstrap [46,47]. The area (AUC) under the receiver (ROC) operating characteristic curve was used to evaluate the model accuracy as a threshold [45]. The value of AUC is between 0 and 1, which is closer to 1 with higher accuracy. The value of AUC is considered as three classification criterion: poor ( $0.5 < AUC \leq 0.7$ ), fair ( $0.7 < AUC \leq 0.9$ ), and excellent ( $0.9 < AUC$ ) [48].

### 2.4. Delineation of Potentially Suitable Habitats (PSH)

We used ArcGIS 10.8 to present the PSH of *E. ceratoniae* under different future climate scenarios predicted by the optimized MaxEnt model. The PSH of *E. ceratoniae* were divided into four grades via the maximum training sensitivity plus specificity threshold: unsuitable habitat ( $0 \leq p \leq 0.1821$ ), poorly suitable habitat ( $0.1821 < p \leq 0.4$ ), moderately suitable habitat ( $0.4 < p \leq 0.6$ ), and highly suitable habitat ( $0.6 < p \leq 1$ ).

We used the “field calculator tool” in ArcGIS 10.8 software to calculate the areas, centroids, and shift trend for *E. ceratoniae* under different future climate scenarios using the “feature to point tool” [49,50].

## 3. Results

### 3.1. Model Performance

We set the RM as 2.0 and the FC as LQHPT to construct the optimal MaxEnt model when  $\Delta AICc$  was 0 through the lambdas file. The mean AUC was 0.972, indicating the MaxEnt model showed excellent performance in predicting the PSH of *E. ceratoniae* (Figure 2).

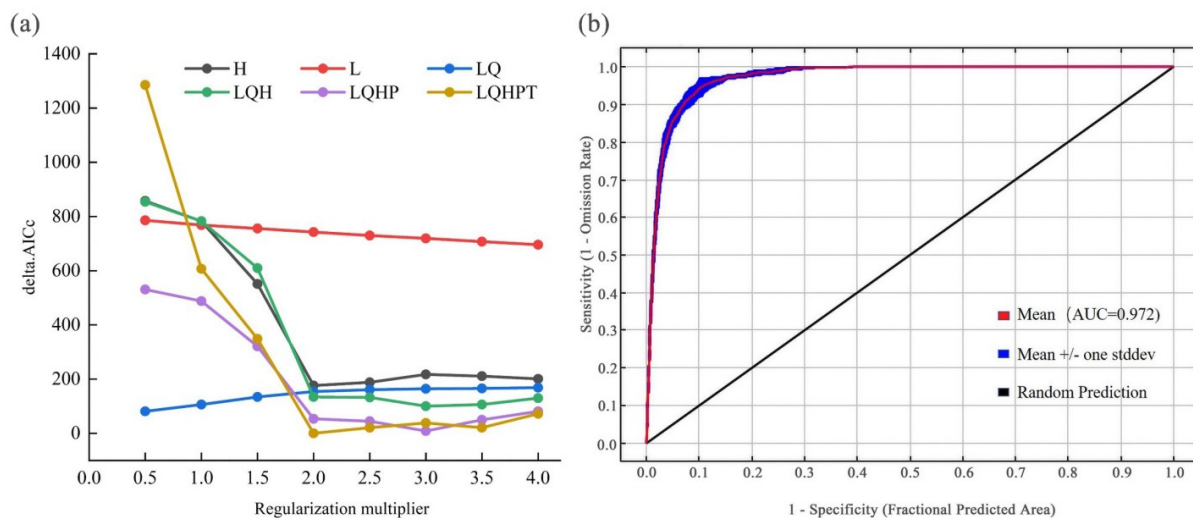
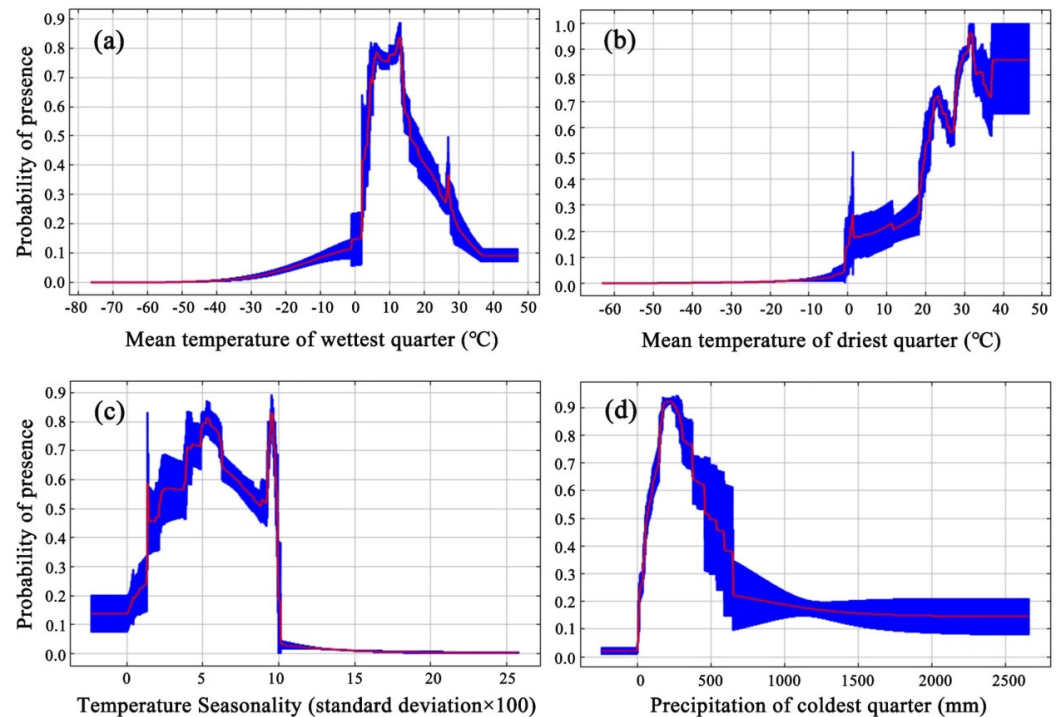


Figure 2. Optimal parameter results for the MaxEnt model (a) and the AUC value (b).

### 3.2. Significant Environmental Variables (EVs)

We screened more significant EVs in the PSH of *E. ceratoniae* based on the contribution of EVs and the “Jackknife method” (Table 1, Figure S2). The total contribution of temperature and precipitation variables achieved 67.1% and 9.1%. Thus, temperature was the most important EVs that influenced the PSH of *E. ceratoniae*. When the probability of presence was higher than 0.6, the range of EVs was preferable to the introduction and establishment of *E. ceratoniae*. Therefore, the suitable ranges of bio9, bio8, bio4, and bio19 were 19.5 to 32.0 °C, 4.3 to 13.5 °C, 226.9 to 620.7, and 147.1 to 373.6 mm, respectively (Figure 3). For bio9, bio8, bio4, and bio19, the best suitable conditions were 31.9 °C, 12.22 °C, 378.8, and 373.6 mm, respectively.



**Figure 3.** Response curves of significant environmental variables (EVs) and the curves show the mean response of the 10 replicate Maxent runs (red) and the mean  $\pm$  one standard deviation (blue, two shades for categorical variables).

### 3.3. Potentially Suitable Habitats under Current Climatic Scenarios

The PSH of *E. ceratoniae* are located mainly in southwestern Asia, northern Africa, and southern Europe under the current climate scenario (Figure 4). The global total, highly, moderately, and poorly suitable habitat areas (SHAs) are about  $1597.65 \times 10^4$ ,  $434.31 \times 10^4$ ,  $348.06 \times 10^4$ , and  $815.19 \times 10^4$  km<sup>2</sup>. The largest total, highly, moderately, and poorly PSH of *E. ceratoniae* was located in Asia (Iran, China, India, and Pakistan), about  $687.57 \times 10^4$ ,  $252.28 \times 10^4$ ,  $156.62 \times 10^4$ , and  $278.67 \times 10^4$  km<sup>2</sup>; followed by Africa (Tunisia, Madagascar, Egypt, and South Africa), about  $307.68 \times 10^4$ ,  $75.65 \times 10^4$ ,  $73.42 \times 10^4$ , and  $158.61 \times 10^4$  km<sup>2</sup>; followed by in Europe (Portugal, France, Italy, and Spain), about  $232.67 \times 10^4$ ,  $62.40 \times 10^4$ ,  $40.34 \times 10^4$ , and  $129.93 \times 10^4$  km<sup>2</sup>.

### 3.4. Potentially Suitable Habitats (PSH) under Future Climatic Conditions

The PSH of *E. ceratoniae* in the 2030s and 2050s under the SSP1-2.6, SSP2-4.5, and SSP5-8.5 scenarios are presented in Figures 5 and 6. Compared to the current climate, the total SHAs of *E. ceratoniae* increased, except in Europe, whereas the poorly SHAs of *E. ceratoniae* decreased to different extents. The PSH of *E. ceratoniae* are primarily concentrated in southeastern India in Asia, northwestern Spain in Europe, and northwestern Brazil in South America.

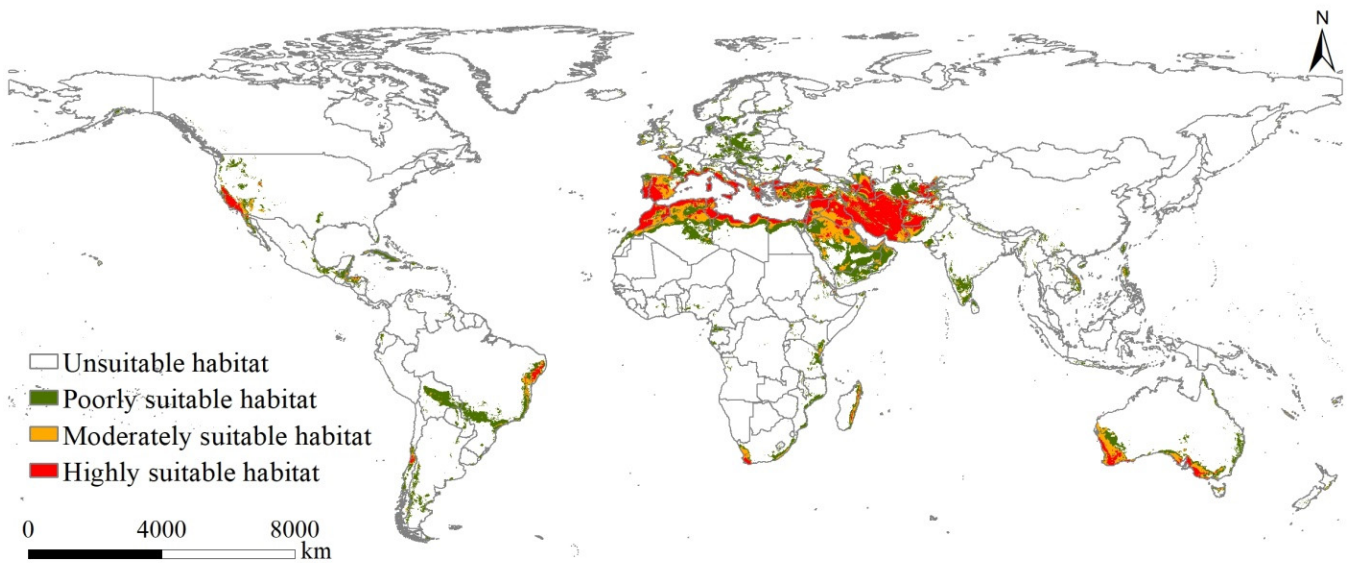


Figure 4. Current global distribution of potentially suitable habitats (PSH) for *Ectomyelois ceratoniae*.

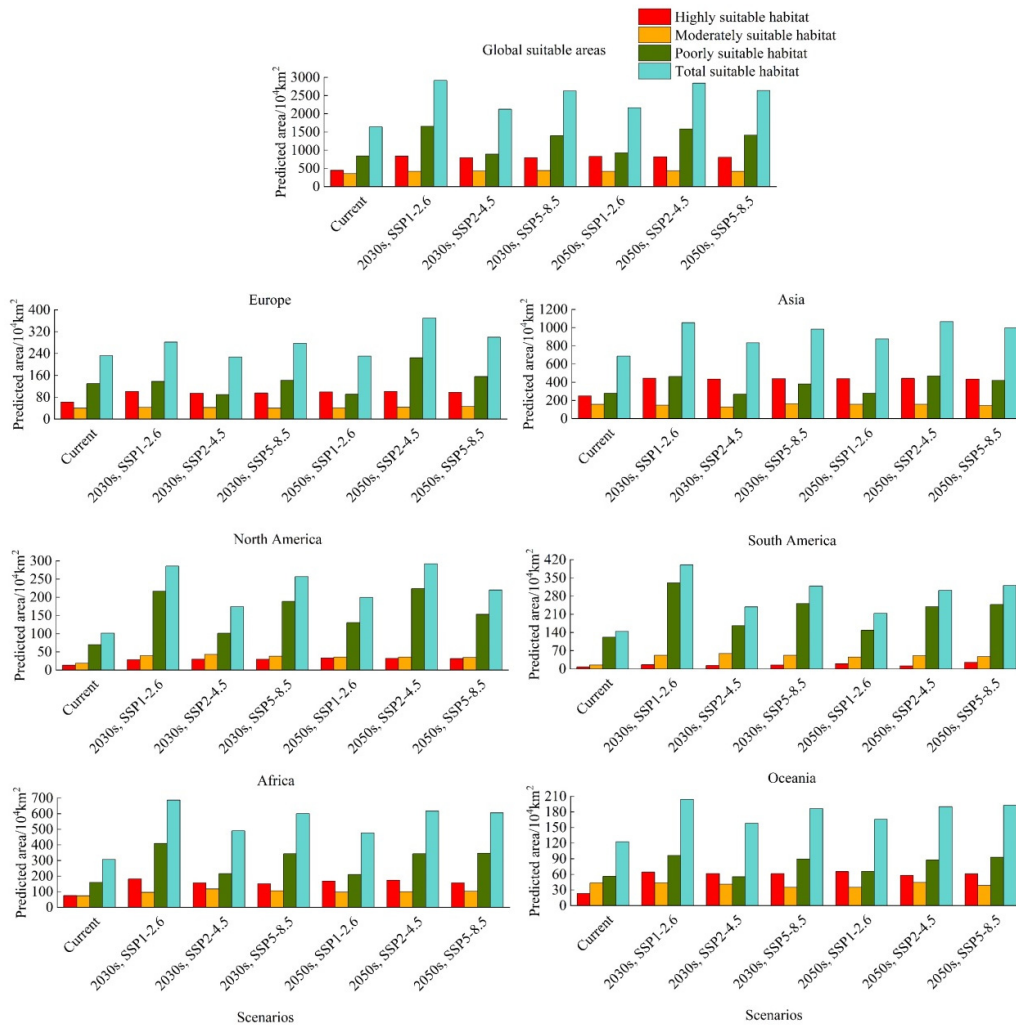
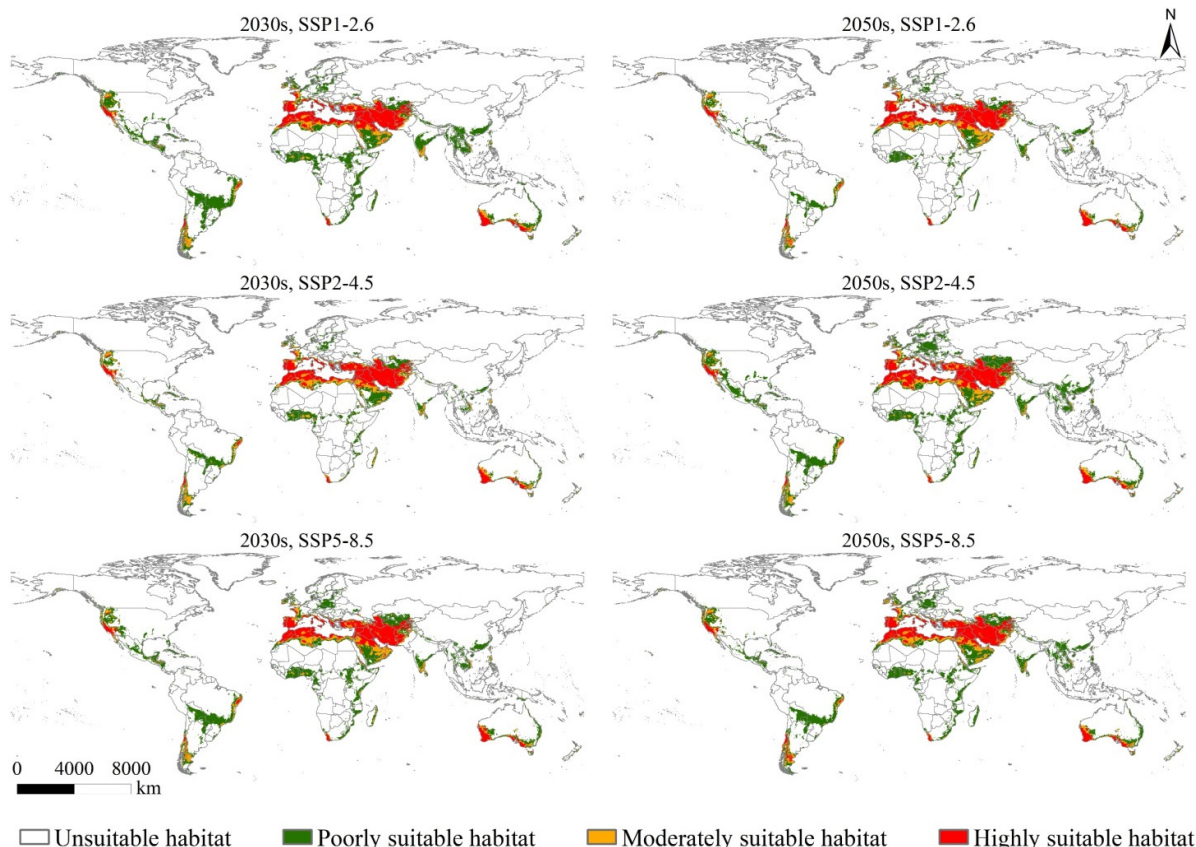


Figure 5. Global potentially suitable habitats (PSH) for *Ectomyelois ceratoniae* under future climate scenarios and potentially suitable habitats (PSH) by continent.



**Figure 6.** Possible future suitable habitats for *Ectomyeloides ceratoniae* based on the various scenarios.

In the 2030s, total, highly, moderately, and poorly SHAs of *E. ceratoniae* showed an increasing trend in South America, with the SHAs of *E. ceratoniae* reaching the maximum under the SSP1-2.6 scenario, about  $400.10 \times 10^4$ ,  $15.99 \times 10^4$ ,  $52.74 \times 10^4$ , and  $331.37 \times 10^4$  km<sup>2</sup>, respectively. The total, highly, moderately, and poorly SHAs of *E. ceratoniae* presented an increasing trend in North America, with the SHAs of *E. ceratoniae* reaching the maximum under the SSP1-2.6 scenario, about  $285.61 \times 10^4$ ,  $28.79 \times 10^4$ ,  $39.72 \times 10^4$ , and  $217.10 \times 10^4$  km<sup>2</sup>, respectively. The total, highly, moderately, and poorly SHAs of *E. ceratoniae* presented an increasing trend in Africa, with the SHAs of *E. ceratoniae* reaching the maximum under the SSP1-2.6 scenario, about  $687.80 \times 10^4$ ,  $181.76 \times 10^4$ ,  $95.93 \times 10^4$ , and  $410.12 \times 10^4$  km<sup>2</sup>, respectively. The total, highly, and poorly SHAs of *E. ceratoniae* showed an increasing trend and moderately SHAs presented a decreasing trend in Oceania, with the SHAs of *E. ceratoniae* reaching the maximum under the SSP1-2.6 scenario, about  $204.42 \times 10^4$ ,  $64.47 \times 10^4$ ,  $43.35 \times 10^4$ , and  $96.60 \times 10^4$  km<sup>2</sup>, respectively. The total, highly, and poorly SHAs of *E. ceratoniae* showed an increasing trend, and moderately SHAs presented a decreasing trend in Asia. The SHAs of *E. ceratoniae* reached the maximum under the SSP1-2.6 scenario, about  $1054.47 \times 10^4$ ,  $444.56 \times 10^4$ ,  $147.27 \times 10^4$ , and  $462.65 \times 10^4$  km<sup>2</sup>, respectively. The total, highly, and moderately SHAs of *E. ceratoniae* presented an increasing trend, and poorly SHAs presented a decreasing trend in Europe; the SHAs of *E. ceratoniae* reached the maximum under the SSP1-2.6 scenario, about  $281.82 \times 10^4$ ,  $101.07 \times 10^4$ ,  $42.98 \times 10^4$ , and  $137.76 \times 10^4$  km<sup>2</sup>, respectively.

In the 2050s, the total, highly, moderately, and poorly SHAs of *E. ceratoniae* present an increasing trend in South America, with the SHAs of *E. ceratoniae* reaching a maximum under the SSP5-8.5 scenario, about  $320.55 \times 10^4$ ,  $25.74 \times 10^4$ ,  $47.33 \times 10^4$ , and  $247.48 \times 10^4$  km<sup>2</sup>, respectively. The total, highly, moderately, and poorly SHAs of *E. ceratoniae* showed an increasing trend in North America, with the SHAs of *E. ceratoniae* reaching a maximum under SSP2-4.5, about  $292.41 \times 10^4$ ,  $32.28 \times 10^4$ ,  $36.02 \times 10^4$ , and  $224.11 \times 10^4$  km<sup>2</sup>, respectively. The total, highly, moderately, and poorly SHAs of *E. cer-*

*atoniae* showed an increasing trend in Africa, with the SHAs of *E. ceratoniae* reaching a maximum under the SSP2-4.5 scenario, about  $616.75 \times 10^4$ ,  $174.29 \times 10^4$ ,  $99.59 \times 10^4$ , and  $342.87 \times 10^4$  km<sup>2</sup>, respectively. The total, highly, and poorly SHAs of *E. ceratoniae* showed an increasing trend and moderately SHAs presented a decreasing trend in Oceania, with the SHAs of *E. ceratoniae* reaching a maximum under the SSP2-4.5 scenario, about  $190.16 \times 10^4$ ,  $58.15 \times 10^4$ ,  $44.52 \times 10^4$ , and  $87.49 \times 10^4$  km<sup>2</sup>, respectively. The total, highly, and poorly SHAs of *E. ceratoniae* showed an increasing trend, and moderately SHAs presented a decreasing trend in Asia; the SHAs of *E. ceratoniae* reached the maximum under the SSP2-4.5 scenario, about  $1068.17 \times 10^4$ ,  $442.56 \times 10^4$ ,  $158.68 \times 10^4$ , and  $466.93 \times 10^4$  km<sup>2</sup>, respectively. The total, highly, and moderately SHAs of *E. ceratoniae* presented an increasing trend, and poorly SHAs presented a decreasing trend in Europe; the SHAs of *E. ceratoniae* reached a maximum under the SSP2-4.5 scenario, about  $369.82 \times 10^4$ ,  $101.44 \times 10^4$ ,  $43.57 \times 10^4$ , and  $224.81 \times 10^4$  km<sup>2</sup>, respectively (Figures 5 and 6).

### 3.5. Potentially Suitable Habitats (PSH) Change

The changes in the SHAs of *E. ceratoniae* in the 2030s and 2050s are shown in Figure 7.

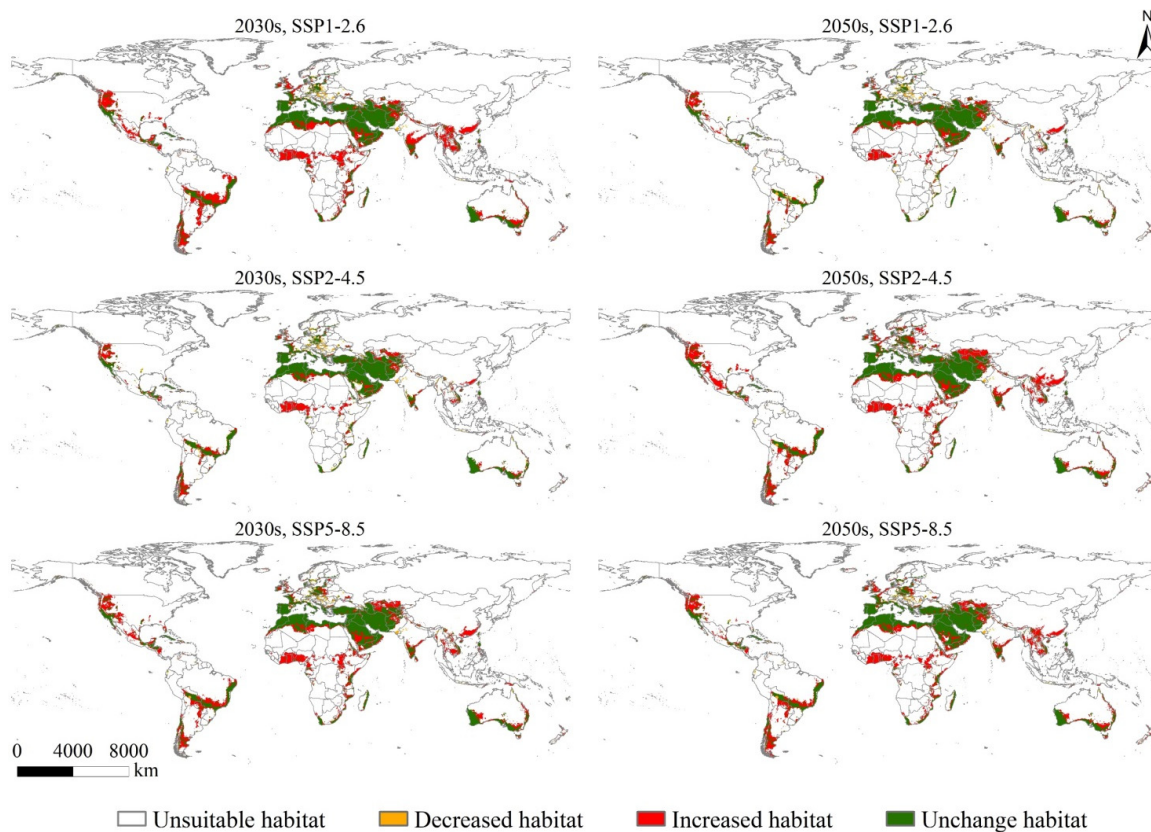


**Figure 7.** Future changes in potentially suitable habitats (PSH) for global *Ectomyelois ceratoniae* for different periods compared to climate conditions in the current period.

In the 2030s, the global total SHAs of *E. ceratoniae* would increase by  $1398.47 \times 10^4$ ,  $652.98 \times 10^4$ , and  $1116.26 \times 10^4$  km<sup>2</sup>, under SSP1-2.6, SSP2-4.5, and SSP5-8.5, respectively. The increased SHAs of *E. ceratoniae* were located in southern China, northeast Iran, southern India in Asia, southeastern Brazil, southwestern Argentina in South America, the northwestern United States of America in North America, southern Australia in Oceania, and northwestern Ethiopia in Africa. Furthermore, the global total SHAs of *E. ceratoniae* would decrease by  $54.45 \times 10^4$ ,  $114.34 \times 10^4$ , and  $59.43 \times 10^4$  km<sup>2</sup>, under SSP1-2.6, SSP2-4.5, and SSP5-8.5, respectively. The decreases in the SHAs of *E. ceratoniae* were located in southeastern India in Asia, northwest Poland in Europe, and northwestern Brazil in South America.

In the 2050s, the global total SHAs of *E. ceratoniae* would increase by  $712.85 \times 10^4$ ,  $1304.21 \times 10^4$ , and  $1128.34 \times 10^4$  km<sup>2</sup>, under SSP1-2.6, SSP2-4.5, and SSP5-8.5, respectively. The increased SHAs of *E. ceratoniae* were located in southern China, northeastern Iran, southern India in Asia, southwestern Argentina in South America, the northwestern United States of America in North America, southern Australia in Oceania, and northwestern Ethiopia in Africa. Furthermore, the global total SHAs of *E. ceratoniae* would decrease by  $126.06 \times 10^4$ ,  $34.30 \times 10^4$ , and  $61.14 \times 10^4$  km<sup>2</sup>, under SSP1-2.6, SSP2-4.5, and SSP5-8.5, respectively. The decreased SHAs of *E. ceratoniae* were located in southeastern India in Asia, northwestern Poland in Europe, northwestern Brazil in South America, and the southwestern United States of America in North America.

### 3.6. Center Transfer

The central transfer of *E. ceratoniae* from the current climate to future climate scenarios is shown in Figure 8. In the current climate, the distribution center of *E. ceratoniae* is located in Iran (49.03° E, 31.99° N). Under SSP1-2.6, the distribution center of *E. ceratoniae* transferred 1308 km to southeast Saudi Arabia (50.70° E, 19.89° N) during the 2030s, and 1955 km to northeast Iran (60.43° E, 35.60° N) during the 2050s. Under SSP2-4.5, the distribution center of *E. ceratoniae* transferred 1130 km to the northeastern Iran (60.55° E, 35.63° N) during the 2030s, and 1930 km to southwestern Saudi Arabia (50.82° E, 19.91° N) during the 2050s. Under SSP5-8.5, the distribution center of *E. ceratoniae* transferred 1203 km to the southern Saudi Arabia (49.69° E, 20.70° N) during the 2030s, and 158 km to southwestern Saudi Arabia (50.73° E, 20.01° N) during the 2050s. The central transfer of *E. ceratoniae* shifted to lower latitudes with climate change.

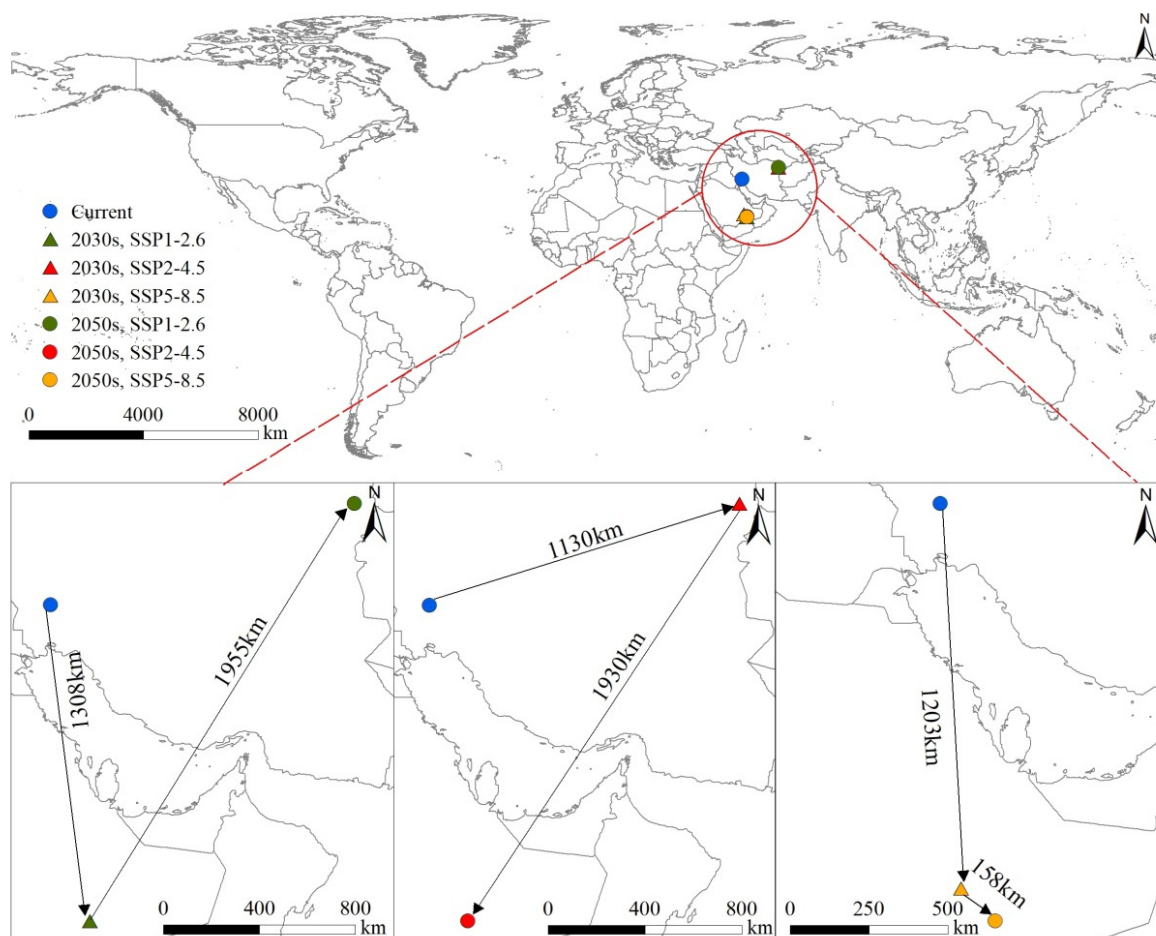


**Figure 8.** Changes in the geographic center of potentially suitable habitats (PSH) of *Ectomyelois ceratoniae* over time.

#### 4. Discussion

*Ectomyelois ceratoniae* has high polyphagia and fecundity that affects hosts such as pomegranate and date palm and causes serious damage to the global fruit industry [7]. Predicting the PSH of *E. ceratoniae* worldwide is important for its prevention, control, and management. Therefore, we used the optimized MaxEnt model to predict the PSH of *E. ceratoniae* worldwide under climate change conditions. Our findings not only provide theoretical guidance for the prevention and control of *E. ceratoniae*, but also ensure the safety of the global fruit industry.

As poikilothermic animals, insects are sensitive to changes in temperature. Warming can directly affect the life history, fitness, and population dynamics of many insects by increasing developmental rates, survival, or fecundity [51]. Therefore, knowing the range of suitable temperatures for insects is of significant importance for their growth and reproduction under climate warming. Previous studies have found that Cox cultured *E. ceratoniae* on maize at different temperatures and humidity and reported total egg development times of 4–5, 3–4, and 3–4 days at 25, 30, and 35 °C, 70–80%, respectively; and the total developmental period from egg hatch to adult emergence at 70% r.h. averaged 48 days at 20 °C, 30 days at 25 °C and 23 days at 30 °C [52]. Exposure to 50 °C for 10 min, 55 °C for 5 min, and 60 °C for 3 min could kill *E. ceratoniae* [53]. Our results are similar to the suitable and lethal temperature of *E. ceratoniae* in previous studies. Our study showed that bio8, bio9, and bio4 were significant biological variables for *E. ceratoniae* development, which shows that the temperature is more suitable at approximately 32 °C and survival is unlikely over 40 °C. These results showed that the development of *E. ceratoniae* responded significantly to temperature changes. Moreover, our results showed that precipitation with below 370 mm is also an important EVs for *E. ceratoniae* growth. Ahmadi et al. showed that Iranian areas where *E. ceratoniae* occurs have an annual rainfall of <200 mm [54]. These studies confirm the accuracy of our findings that temperature and precipitation have a significant effect on the survival of *E. ceratoniae*.

Predicting the PSH of invasive alien species with climate warming is an important part of early warming and species management. Previous studies have shown that the PSH of *Deanolis sublimbalis* (Snellen) worldwide has a relative increase under climate change [55]. Our results are consistent with the trend that the PSH of *E. ceratoniae* is relatively increased under current and future climatic conditions, where it is mainly distributed in southern Europe, northern Africa, and most of southwestern Asia (Tunisia, Iran and China). This is consistent with *E. ceratoniae* being suitable for survival in hot and dry climates. Furthermore, previous studies have shown that pomegranate with over 200 cultivars and cultivated in China for over 2000 years, located mainly in Shandong, Xinjiang, and Yunnan provinces [56], as well as Shahvare-Danese fid, is a pomegranate cultivar relatively susceptible to *E. ceratoniae* [8]. The increased PSH of *E. ceratoniae* cover the main pomegranate production area, which is suitable for the survival and reproduction of *E. ceratoniae* [7]. Therefore, countries in southwest Asia should take care to prevent damage from *E. ceratoniae*.

*Ectomyelois ceratoniae* can spread over short distances by wind, and over long distances by flight in fruits, such as pomegranates, dates, and pistachios [23]. Therefore, the regions of increase under future climatic scenarios—particularly Iran, Argentina, the United States, and Australia, which have large increases in area—should be alert to host plant introductions and strengthen early warnings and management to prevent the further spread of secondary invasions of *E. ceratoniae*. Furthermore, *E. ceratoniae* has spread globally with increased global trade, and some of the major fruit-producing regions—including the world's major pomegranate growing areas such as China, the United States, Australia, and Iran—are suitable for *E. ceratoniae*, posing potential economic loss and production damage for the global fruit industry. *Ectomyelois ceratoniae* is widely spread throughout southern Europe, northern Africa, and southwestern Asia. Based on the invasion risks mentioned above, these countries should firstly strengthen early warnings of *E. ceratoniae*, and adopt effective control measures to eradicate it, such as cultural, chemical, and biological measures. Cultural measures include the prompt disposal of dropped and left-on-tree fruit [57]. Chemical measures

often involve using insecticides, such as cypermethrin and emamectin benzoate [58]. Biological measures involve infecting the *E. ceratoniae* with *Bacillus thuringiensis* (Berliner) [59]. Although these control measures can prevent *E. ceratoniae* from harming the host plant, they all have shortcomings, including the long duration of cultural measures, the risk of damage to the crop itself from chemical measures, and the long research cycle for implementing pre-biological measures. Therefore, early warning, monitoring, prevention, control, and management systems should be established to prevent further harm from *E. ceratoniae*.

## 5. Conclusions

In this study, we used the MaxEnt model to predict the PSH of *E. ceratoniae* based on 228 records of global geographic distribution and nine environmental factors. Temperature was the most important EVs of significance influencing its distribution (bio9 and bio8). Under current climate, the PSH of *E. ceratoniae* were in southern Europe, northern Africa, and southwestern Asia. Under future climate scenarios, the PSH of *E. ceratoniae* showed an overall increasing trend, with an increase in areas mainly located in southwest Asia (China, Iran, Afghanistan, and India). Therefore, the main pomegranate production areas, such as China and Iran, should strengthen quarantine, prevention, and control measures to prevent the continuous spread and invasion of *E. ceratoniae*. Control measures such as the prompt disposal of fallen and residual fruits on the trees, bagging of fruits, and the use of cypermethrin insecticides are considered efficient measures to eliminate this pest. Thus, our study could provide a theoretical foundation for the treatment and control of *E. ceratoniae*.

**Supplementary Materials:** The following supporting information can be downloaded at: <https://www.mdpi.com/article/10.3390/atmos15010119/s1>, Figure S1: Correlation analysis of environmental factors; Figure S2: Graph of the results of the Jackknife method; Table S1: Bioclimatic variables are related to the distribution of *Ectomyelois ceratoniae*.

**Author Contributions:** Conceptualization, C.L., M.Y. and W.L.; methodology, C.L.; software, M.Y.; validation, C.L. and M.Y.; formal analysis, C.L. and M.Y.; investigation, C.L., M.Y. and Z.J.; resources, M.Y. and N.Y.; data curation, C.L. and Z.J.; writing—original draft preparation, C.L. and M.Y.; writing—review and editing, C.L., M.Y., M.L., Z.J., H.Y. and W.L.; visualization, C.L., M.Y., M.L. and N.Y.; supervision, C.L. and M.Y.; project administration, W.L.; funding acquisition, W.L. All authors have read and agreed to the published version of the manuscript.

**Funding:** This research was funded by the National Key R&D Program of China (Grant No. 2021YFC2600400) and Technology Innovation Program of Chinese Academy of Agricultural Sciences (Grant No. caascx-2022-2025-IAS).

**Institutional Review Board Statement:** This study did not involve humans or animals.

**Informed Consent Statement:** Not applicable.

**Data Availability Statement:** The data presented in this study are openly available in GBIF at <https://doi.org/10.15468/dl.73j6ct>; accessed on 26 August 2022. Current climate and future climate data were downloaded from the WorldClim database (<https://www.worldclim.org/>, accessed on 26 August 2022).

**Conflicts of Interest:** The authors declare no conflicts of interest.

## References

1. Gentili, R.; Schaffner, U.; Martinoli, A.; Citterio, S. Invasive alien species and biodiversity: Impacts and management. *Biodiversity* **2021**, *22*, 1–3. [[CrossRef](#)]
2. Kenis, M.; Auger-Rozenberg, M.-A.; Roques, A.; Timms, L.; P  r  , C.; Cock, M.J.W.; Settele, J.; Augustin, S.; Lopez-Vaamonde, C. Ecological effects of invasive alien insects. *Biol. Invasions* **2009**, *11*, 21–45. [[CrossRef](#)]
3. Klem, C.C.; Zaspel, J. Pest Injury Guilds, Lepidoptera, and Placing Fruit-Piercing Moths in Context: A Review. *Ann. Entomol. Soc. Am.* **2019**, *112*, 421–432. [[CrossRef](#)]
4. Njuguna, E.; Nethononda, P.; Maredia, K.; Mbabazi, R.; Kachapulula, P.; Rowe, A.; Ndolo, D. Experiences and Perspectives on *Spodoptera frugiperda* (Lepidoptera: Noctuidae) Management in Sub-Saharan Africa. *J. Integr. Pest Manag.* **2021**, *12*, 7. [[CrossRef](#)]

5. Singh, S.; Kaur, G.; Onkara Naik, S.; Rami Reddy, P.V. The Shoot and Fruit Borer, *Conogethes punctiferalis* (Guenee): An Important Pest of Tropical and Subtropical Fruit Crops. In *The Black Spotted, Yellow Borer, Conogethes Punctiferalis Guenée and Allied Species*; Chakravarthy, A.K., Ed.; Springer: Singapore, 2018; pp. 165–191.
6. Ahmad, R.; Khuroo, A.A.; Charles, B.; Hamid, M.; Rashid, I.; Aravind, N.A. Global distribution modelling, invasion risk assessment and niche dynamics of *Leucanthemum vulgare* (Ox-eye Daisy) under climate change. *Sci. Rep.* **2019**, *9*, 11395. [[CrossRef](#)] [[PubMed](#)]
7. Dueñas-López, M.A. *Ectomyelois Ceratoniae* (Carob Moth); CABI Compendium; CABI International: Wallingford, UK, 2022; p. 11. [[CrossRef](#)]
8. Abedi, Z.; Golizadeh, A.; Soufbaf, M.; Hassanpour, M.; Jafari-Nodoushan, A.; Akhavan, H.-R. Relationship between Performance of Carob Moth, *Ectomyelois ceratoniae* Zeller (Lepidoptera: Pyralidae) and Phytochemical Metabolites in Various Pomegranate Cultivars. *Front. Physiol.* **2019**, *10*, 1425. [[CrossRef](#)] [[PubMed](#)]
9. Heinrich, C. American moths of the subfamily Phycitinae. *Bulletin* **1956**, *207*, 581.
10. Abedi, Z.; Golizadeh, A.; Hassanpour, M.; Soufbaf, M. Performance of *Habrobracon hebetor* (Say) (Hymenoptera: Braconidae) parasitizing *Ectomyelois ceratoniae* (Zeller) (Lepidoptera: Pyralidae) on different pomegranate cultivars. *Int. J. Trop. Insect Sci.* **2021**, *41*, 95–105. [[CrossRef](#)]
11. Mehrnejad, M. The current status of pistachio pests in Iran. *Cah. Options Méditerranéennes* **2001**, *56*, 315–322.
12. Braham, M. Insect larvae associated with dropped pomegranate fruits in an organic orchard in Tunisia. *J. Entomol. Nematol.* **2015**, *7*, 5–10. [[CrossRef](#)]
13. Perring, T.M.; El-Shafie, H.A.F.; Wakil, W. Carob Moth. In *Sustainable Pest Management in Date Palm: Current Status and Emerging Challenges*; Wakil, W., Romeno Faleiro, J., Miller, T.A., Eds.; Springer International Publishing: Cham, Switzerland, 2015; pp. 109–167.
14. Al-Izzi, M.A.J.; Al-Maliky, S.K.; Younis, M.A.; Jabbo, N.F. Bionomics of *Ectomyelois ceratoniae* (Lepidoptera: Pyralidae) on Pomegranates in Iraq. *Environ. Entomol.* **1985**, *14*, 149–153. [[CrossRef](#)]
15. Warner, R.L.; Barnes, M.M.; Laird, E.F. Chemical Control of a Carob Moth, *Ectomyelois ceratoniae* (Lepidoptera: Pyralidae), and Various Nitidulid Beetles (Coleoptera) on ‘Deglet Noor’ Dates in California. *J. Econ. Entomol.* **1990**, *83*, 2357–2361. [[CrossRef](#)]
16. Hosseini, S.A.; Goldansaz, S.H.; Fotoukkaia, S.M.; Menken, S.B.J.; Groot, A.T. Seasonal pattern of infestation by the carob moth *Ectomyelois ceratoniae* in pomegranate cultivars. *Crop Prot.* **2017**, *102*, 19–24. [[CrossRef](#)]
17. Warner, R.L.; Barnes, M.M.; Laird, E.F. Reduction of Insect Infestation and Fungal Infection by Cultural Practice in Date Gardens. *Environ. Entomol.* **1990**, *19*, 1618–1623. [[CrossRef](#)]
18. Vetter, R.S.; Tatevossian, S.; Baker, T. Reproductive behavior of the female carob moth, (Lepidoptera: Pyralidae). *Pan-Pac. Entomol.* **1997**, *73*, 28–35.
19. Solis, M. Key to Selected Pyraloidea (Lepidoptera) Larvae Intercepted at U. S. Ports of Entry: Revision of Pyraloidea in “Keys to Some Frequently Intercepted Lepidopterous Larvae” by Weisman 1986 (Updated 2006). *Proc. Entomol. Soc. Wash.* **2006**, *101*.
20. Wang, B.-X.; Zhu, L.; Ma, G.; Najjar-Rodriguez, A.; Zhang, J.-P.; Zhang, F.; Avila, G.A.; Ma, C.-S. Current and Potential Future Global Distribution of the Raisin Moth *Cadra figulilella* (Lepidoptera: Pyralidae) under Two Different Climate Change Scenarios. *Biology* **2023**, *12*, 435. [[CrossRef](#)]
21. Zhu, H.; Kumar, S.; Neven, L.G. Codling Moth (Lepidoptera: Tortricidae) Establishment in China: Stages of Invasion and Potential Future Distribution. *J. Insect. Sci.* **2017**, *17*, 85. [[CrossRef](#)]
22. Khodabakhshian, R.; Emadi, B.; Khojastehpour, M.; Golzarian, M.R. Carob moth, *Ectomyelois ceratoniae*, detection in pomegranate using visible/near infrared spectroscopy. *Comput. Electron. Agric.* **2016**, *129*, 9–14. [[CrossRef](#)]
23. Abid, I.; Laghfiri, M.; Bouamri, R.; Aleya, L.; Bouriou, M. Integrated pest management (IPM) for *Ectomyelois ceratoniae* on date palm. *Curr. Opin. Environ. Sci. Health* **2021**, *19*, 100219. [[CrossRef](#)]
24. Ranjbar, M.; Zibae, A.; Sendi, J.J. Purification and characterization of a digestive lipase in the midgut of *Ectomyelois ceratoniae* Zeller (Lepidoptera: Pyralidae). *Front. Life Sci.* **2015**, *8*, 64–70. [[CrossRef](#)]
25. Alotaibi, S.S.; Darwish, H.; Zaynab, M.; Alharthi, S.; Alghamdi, A.; Al-Barty, A.; Asif, M.; Wahdan, R.H.; Baaeeem, A.; Noureldeen, A. Isolation, Identification, and Biocontrol Potential of Entomopathogenic Nematodes and Associated Bacteria against *Virachola livia* (Lepidoptera: Lycaenidae) and *Ectomyelois ceratoniae* (Lepidoptera: Pyralidae). *Biology* **2022**, *11*, 295. [[CrossRef](#)] [[PubMed](#)]
26. Morland, G. The morphology and ecology of the Carob moth (*Ectomyelois ceratoniae*) (Zeller) in citrus orchards of the Western Cape, South Africa. Ph.D. Thesis, Stellenbosch University, Stellenbosch, South Africa, 2015.
27. Leyequien, E.; Verrelst, J.; Slot, M.; Schaepman-Strub, G.; Heitkonig, I.; Skidmore, A. Capturing the fugitive: Applying remote sensing to terrestrial animal distribution and diversity. *Int. J. Appl. Earth Obs. Geoinf.* **2007**, *9*, 1–20. [[CrossRef](#)]
28. Lodge, D.M.; Simonin, P.W.; Burgiel, S.W.; Keller, R.P.; Bossenbroek, J.M.; Jerde, C.L.; Kramer, A.M.; Rutherford, E.S.; Barnes, M.A.; Wittmann, M.E.; et al. Risk Analysis and Bioeconomics of Invasive Species to Inform Policy and Management. *Annu. Rev. Environ. Resour.* **2016**, *41*, 453–488. [[CrossRef](#)]
29. Thapa, A.; Wu, R.; Hu, Y.; Nie, Y.; Singh, P.B.; Khatiwada, J.R.; Yan, L.; Gu, X.; Wei, F. Predicting the potential distribution of the endangered red panda across its entire range using MaxEnt modeling. *Ecol. Evol.* **2018**, *8*, 10542–10554. [[CrossRef](#)] [[PubMed](#)]
30. Carpenter, G.; Gillison, A.N.; Winter, J. Domain: A flexible modelling procedure for mapping potential distributions of plants and animals. *Biodivers. Conserv.* **1993**, *2*, 667–680. [[CrossRef](#)]
31. Busby, J.R. Bioclim—A bioclimate analysis and prediction system. *Plant Prot. Q.* **1991**, *61*, 8–9.
32. Jie, L.; Yang, J.-B.; Li, W. Potential distribution analysis of an invasive alien species *Parapediasia teterrella* (Lepidoptera, Crambidae) in East Asia. *J. Asia-Pac. Entomol.* **2020**, *23*, 219–223. [[CrossRef](#)]

33. San Blas, G.; Obholz, G.; Dias, F.; Specht, A.; Casagrande, M.; Mielke, O. Global Potential Distribution of the South American Cutworm Pest *Agrotis robusta* (Lepidoptera: Noctuidae). *Neotrop. Entomol.* **2022**, *51*, 198. [[CrossRef](#)] [[PubMed](#)]
34. Elith, J.; Leathwick, J.R. Species Distribution Models: Ecological Explanation and Prediction across Space and Time. *Annu. Rev. Ecol. Evol. Syst.* **2009**, *40*, 677–697. [[CrossRef](#)]
35. Stockwell, D. The GARP modelling system: Problems and solutions to automated spatial prediction. *Int. J. Geogr. Inf. Sci.* **1999**, *13*, 143–158. [[CrossRef](#)]
36. Muscarella, R.; Galante, P.J.; Soley-Guardia, M.; Boria, R.A.; Kass, J.M.; Uriarte, M.; Anderson, R.P. ENMeval: An R package for conducting spatially independent evaluations and estimating optimal model complexity for Maxent ecological niche models. *Methods Ecol. Evol.* **2014**, *5*, 1198–1205. [[CrossRef](#)]
37. Fotheringham, A.; Oshan, T. Geographically weighted regression and multicollinearity: Dispelling the myth. *J. Geogr. Syst.* **2016**, *18*, 303–329. [[CrossRef](#)]
38. GBIF.org (26 August 2022) GBIF Occurrence Download. Available online: <https://doi.org/10.15468/dl.73j6ct> (accessed on 26 August 2022).
39. Warren, D.L.; Glor, R.E.; Turelli, M. ENMTools: A toolbox for comparative studies of environmental niche models. *Ecography* **2010**, *33*, 607–611. [[CrossRef](#)]
40. Fick, S.E.; Hijmans, R.J. WorldClim 2: New 1-km spatial resolution climate surfaces for global land areas. *Int. J. Climatol.* **2017**, *37*, 4302–4315. [[CrossRef](#)]
41. Gao, R.; Liu, L.; Zhao, L.; Cui, S. Potentially Suitable Geographical Area for *Monochamus alternatus* under Current and Future Climatic Scenarios Based on Optimized MaxEnt Model. *Insects* **2023**, *14*, 182. [[CrossRef](#)]
42. Ning, Y.; Lei, J.R.; Song, X.Q.; Han, S.M.; Zhong, Y.F. Modeling the potential suitable habitat of *Impatiens hainanensis*, a limestone-endemic plant. *Chin. J. Plant Ecol.* **2018**, *42*, 946–954. [[CrossRef](#)]
43. Sillero, N. What does ecological modelling model? A proposed classification of ecological niche models based on their underlying methods. *Ecol. Model.* **2011**, *222*, 1343–1346. [[CrossRef](#)]
44. Akaike, H. Information Theory and an Extension of the Maximum Likelihood Principle. In *Selected Papers of Hirotugu Akaike*; Parzen, E., Tanabe, K., Kitagawa, G., Eds.; Springer: New York, NY, USA, 1998; pp. 199–213.
45. Ben-David, A. About the relationship between ROC curves and Cohen’s kappa. *Eng. Appl. Artif. Intell.* **2008**, *21*, 874–882. [[CrossRef](#)]
46. Phillips, S.J.; Anderson, R.P.; Dudík, M.; Schapire, R.E.; Blair, M.E. Opening the black box: An open-source release of Maxent. *Ecography* **2017**, *40*, 887–893. [[CrossRef](#)]
47. Altamiranda-Saavedra, M.; Amat, E.; Gómez-P, L.-M. Influence of montane altitudinal ranges on species distribution models; evidence in Andean blow flies. *PeerJ* **2020**, *8*, e10370. [[CrossRef](#)] [[PubMed](#)]
48. Franklin, J. *Mapping Species Distributions: Spatial Inference and Prediction*; Cambridge University Press: Cambridge, UK, 2010. [[CrossRef](#)]
49. Lei, X.; Chen, J.; Zhu, Z.; Guo, X.; Liu, P.; Jiang, X. How to locate urban–rural transit hubs from the viewpoint of county integration? *Phys. A Stat. Mech. Its Appl.* **2022**, *606*, 128148. [[CrossRef](#)]
50. Huang, X.F. *The Study of Landuse Change and Ecological Suitability in Pudong New Area*; East China Normal University: Shanghai, China, 2009.
51. Frank, S.D. Review of the direct and indirect effects of warming and drought on scale insect pests of forest systems. *For. Int. J. For. Res.* **2021**, *94*, 167–180. [[CrossRef](#)]
52. Cox, P.D. The influence of temperature and humidity on the life-cycle of *Ectomyelois ceratoniae* (Zeller) (Lepidoptera: Phycitidae). *J. Stored Prod. Res.* **1976**, *12*, 111–117. [[CrossRef](#)]
53. Ben-Amor, R.; Dhoubi, M.H.; Aguayo, E. Hot water treatments combined with cold storage as a tool for *Ectomyelois ceratoniae* mortality and maintenance of Deglet Noor palm date quality. *Postharvest Biol. Technol.* **2016**, *112*, 247–255. [[CrossRef](#)]
54. Ahmadi, B.; Moharrampour, S.; Sinclair, B.J. Overwintering biology of the carob moth *Apomyelois ceratoniae* (Lepidoptera: Pyralidae). *Int. J. Pest Manag.* **2016**, *62*, 69–74. [[CrossRef](#)]
55. Baradevanal, G.; Chander, S.; Jayanthi, P.D.K.; Singh, H.S.; Reddy, D.S. Assessing the risk of mango quarantine pest *Deanolis sublimbalis* Snellen under different climate change scenarios. *J. Plant Dis. Prot.* **2021**, *128*, 853–863. [[CrossRef](#)]
56. Mellado-Negrete, A.; Peña-Vázquez, G.I.; Urías-Orona, V.; De La Garza, A.L. Polyphenol Bioaccessibility and Antioxidant Activity of Pomegranate (*Punica granatum*) Peel Supplementation in Diet-Induced Obese Rats. *J. Med. Food* **2023**, *26*, 570–579. [[CrossRef](#)]
57. Park, J.-J.; Perring, T. Development of a Binomial Sampling Plan for the Carob Moth (Lepidoptera: Pyralidae), a Pest of California Dates. *J. Econ. Entomol.* **2010**, *103*, 1474–1482. [[CrossRef](#)]
58. Hached, W.; Romdhane, S.; Sahraoui, H.; Lebdi, K. Control trials against *Ectomyelois ceratoniae* Zeller 1881 (Lepidoptera: Pyralidae) under controlled conditions and in citrus orchard. *J. New Sci. Agric. Biotechnol.* **2018**, *49*, 2961–2970.
59. Mnif, I.; Elleuch, M.; Châabouni, S.E.; Ghribi, D.J.C.P. *Bacillus subtilis* SPB1 biosurfactant: Production optimization and insecticidal activity against the carob moth *Ectomyelois ceratoniae*. *Crop Prot.* **2013**, *50*, 66–72. [[CrossRef](#)]

**Disclaimer/Publisher’s Note:** The statements, opinions and data contained in all publications are solely those of the individual author(s) and contributor(s) and not of MDPI and/or the editor(s). MDPI and/or the editor(s) disclaim responsibility for any injury to people or property resulting from any ideas, methods, instructions or products referred to in the content.